

## Gas Sensing Properties of ZnO-SnO<sub>2</sub> Nanocomposite

PUSHPENDRA KUMAR\* and DEEPAK KUMAR

Department of Chemistry, Lovely Professional University, Phagwara-144411, India

\*Corresponding author: E-mail: pushpendra.kmr1@gmail.com

Received: 8 June 2019;

Accepted: 20 July 2019;

Published online: 18 November 2019;

AJC-19673

In present study, ZnO-SnO<sub>2</sub> nanocomposite was synthesized by co-precipitation method and its sensing properties with respect to carbon monoxide gas were investigated. X-ray diffraction pattern shows the exhaustive evolution of hexagonal wurtzite phase of ZnO and rutile phase of SnO<sub>2</sub>. Morphological study was done by FE-SEM and optical characterization was done by UV-visible spectrophotometer. To study the sensing properties, material was layered on conducting substrate and resistance was recorded in the presence of air and CO gas at different operating temperature. Sensing responses of pure ZnO and ZnO-SnO<sub>2</sub> composite was also compared. ZnO-SnO<sub>2</sub> showed much enhanced response along with better response and recovery time compared to pure ZnO.

**Keywords:** ZnO-SnO<sub>2</sub> nanocomposite, CO sensor.

### INTRODUCTION

Carbon monoxide is one of the most polluted gases causing enormous damage and global warming in atmosphere and can be considered as silent killer due to its toxic properties. Therefore, regular monitoring of CO formation is required which is difficult as it is colourless and tasteless [1].

Detection technology based on metal oxide semiconductors has advantage over conventional methods like gas chromatography, mass spectrometer, surface acoustic wave (SAW), selected ion flow tube (SIFT) methods which are limited due to their size, cost and time consuming processing steps [2]. Various sensors are available in market but solid-state reductive gas sensor are attractive due to low cost, easy to fabricate, can be modified at molecular level, high sensitivity and compatible to electrical devices [3].

Many semiconductors like ZnO, TiO<sub>2</sub>, SnO<sub>2</sub>, NiO, V<sub>2</sub>O<sub>5</sub> have been used to detect different gases and volatile compounds [4-8]. However, the selectivity of gas, sensor response to gas and high operating temperature are still a matter of concern. Sensor response depends on the change in resistivity/conductivity caused due to interaction between surrounding environment and metal oxide and hence, selection of metal oxide is an important criterion for active sensors [9].

Transparent ZnO having wide band gap and SnO<sub>2</sub> have been extensively used for many optoelectronics applications due to its unique physical and chemical properties [10]. It shows high variation in electrical conductivity/ resistivity when exposed to the reductive gases. In most of the studies, the operating temperature is much higher than room temperature and efforts are required to fabricate the sensing material which can operate comparatively at low temperature having fast response/recovery time and low detection limits [11,12]. Various modification tools have been adopted to induce favourable properties in material like doping, composites, nanostructures, metal loading, *etc.* [13]. Doping has been reported a tailoring tool to increase the sensitivity at low operating temperature. Doping introduces a intraband gap states along with modification in electrical, structural and morphological characteristics [14]. It also influences the morphology and surface to volume ratio for better adsorption of gaseous molecules [12]. Now days the research has been turned upto composite material having more than one phase having combined favourable properties [15,16]. Synergistic effect of different favourable properties by combing two different materials may lead to better sensing response as it provide more surface active sites for sensing. Heteronanostructures have interfacial contact effects which promotes the charge transfer changes enhancing sensing properties. Fermi

level at the interface of heterostructure get equilibrate at same level, resulting in charge transfer and formation of charge depletion layer which may lead to enhanced gas sensing [13]. Khorami *et al.* [17] synthesized SnO<sub>2</sub>/ZnO composite nanofibers for ethanol sensing which showed better sensor response at lower operating temperature (280 °C) compared to reported operating temperature for ZnO and SnO<sub>2</sub> (above 300 °C). Recovery and response time was also improved. Many studies [10,18,19] reported that sensing properties can be improved by using composite metal oxides.

Pure semiconductors shows high resistance but heterostructures are intended to improve electrical conduction due to increase in number of charge carriers and carrier mobility of the composite [14]. Improved sensing properties of nanocomposites have been attributed to band banding, depletion layer manipulation, synergistic surface reactions, more surface active sites and charge carrier separation [13,19]. Pure ZnO has been widely studied for sensing different gases but it has certain disadvantages like poor selectivity, low response and higher working temperature [16]. Reports indicates that ZnO combined with another suitable material show better sensing properties compared to pure ZnO. In the present work, ZnO-SnO<sub>2</sub> is synthesized by co-precipitation method. When compared to pure ZnO, it was found that ZnO-SnO<sub>2</sub> complex has better sensing response.

## EXPERIMENTAL

Zinc acetate dihydrate was dissolved in distilled water and pH of the solution was maintained at 10 by using ammonia solution. The solution was stirred for 3 h at room temperature. The solution was transferred to Teflon lined sealed autoclave and kept at 80 °C in oven for 12 h. White precipitate was obtained which was washed with distilled water for many times and then subjected to annealing at 500 °C in air. To make the composite zinc acetate dihydrate and tin chloride were taken in similar proportion and same procedure was followed as mentioned above and whitish yellow precipitate was obtained.

Microstructural properties of zinc oxide and zinc oxide-tin oxide composites were evaluated by using XRD (Bruker D8 Advance) and SEM-EDAX (FESEM; JEOLJSM- 7610F plus). Optical absorption was recorded by UV-visible spectroscopy (Shimadzu UV-1800).

To fabricate the sensor, slurry of prepared material in de-ionized water was prepared and coated on ITO conductive glass by doctor blade method and then dried at 400 °C. Sensing properties were analysed by measuring the resistance of ZnO and ZnO-SnO<sub>2</sub> films in presence of carbon monoxide and air (as reference) in air tight steel chamber connected to two probe system. Sensing responses were evaluated at different temperature and concentration by using a expression  $S = R_a/R_g$  ( $R_a$  = resistance in air,  $R_g$  = resistance in gas) [20].

## RESULTS AND DISCUSSION

ZnO-SnO<sub>2</sub> nanocomposite was prepared by sol-gel co-precipitation method. To determine the prepared phase of the compound and crystallinity, the samples were subjected to XRD analysis. Fig. 1 shows the X-ray diffraction pattern in which exhaustive evolution of hexagonal wurtzite phase of ZnO

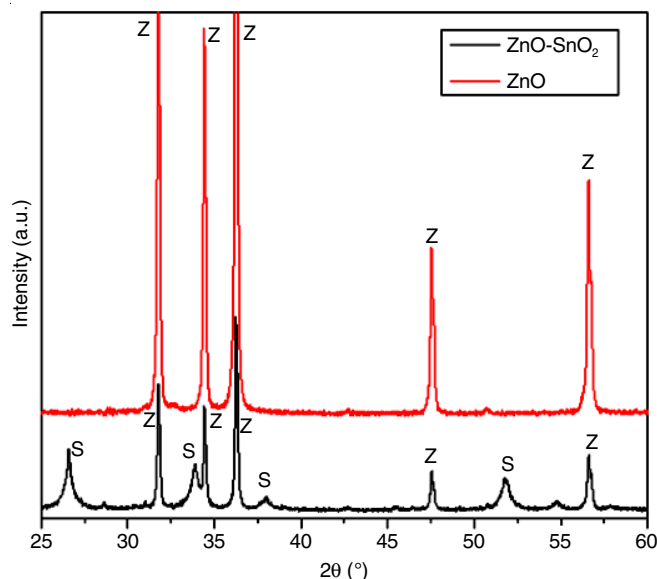


Fig. 1. X-ray diffraction pattern of ZnO and ZnO-SnO<sub>2</sub>

and tetragonal rutile phase of SnO<sub>2</sub> can be seen. Peaks at 2 $\theta$  values 31.79 (100), 34.43 (002), 36.19 (101), 47.57 (102) and 56.57 (110) correspond to hexagonal wurtzite phase of ZnO (JCPDS No. 36-1451) while peaks at 2 $\theta$  values 26.67 (110), 33.93 (101), 38.04 (200), 51.78 (211) and 54.80 (220) correspond to cassiterite crystal phase of SnO<sub>2</sub> with tetragonal rutile structure (JCPDS No. 41-1445). In case of pure ZnO, the intensities of peaks are very high compared to ZnO-SnO<sub>2</sub> which confirms that pure ZnO is well crystalline and on Sn incorporation intensity of peaks reduced remarkably indicating significant reduce in crystallinity. This reduction in crystallinity can be attributed to formation of SnO<sub>2</sub> along with ZnO. Depending upon ionic radii, upto one particular limit the host lattice can accommodate foreign particle but beyond that the foreign particle produce the lattice strain in host lattice resulting reduced crystallinity [21]. Ionic radii of Sn<sup>2+</sup> is 118 pm is much higher than that of Zn<sup>2+</sup> (74 pm) and therefore incorporation of Sn<sup>2+</sup> in ZnO crystal lattice may lead to poor crystallinity. The crystalline size of prepared material was calculated by Scherrer's equation. Average crystalline size of pure ZnO was in the range 26-32 nm while that of ZnO-SnO<sub>2</sub> was in the range 15-20 nm.

Optical absorption was recorded using UV-visible spectrophotometer. To record the spectra synthesized powder was dispersed in ethanol and sonicated for 15 min. Both the samples showed strong optical absorption in UV region (Fig. 2). Optical absorption in ZnO-SnO<sub>2</sub> was more compared to pure ZnO. However, in case of ZnO-SnO<sub>2</sub>, blue shift was also observed.

Fig. 3 shows the morphological structures of synthesized material. In case of pure ZnO very fine spherical granules with clear grain boundaries can be seen. Honeycomb like structure was observed in which small crystals combined to form a big crystal. In case ZnO-SnO<sub>2</sub>, very small crystals can be seen (in the range of 12-18 nm) and are in good agreement to the crystalline size calculated by XRD. Compared to pure ZnO, porosity of ZnO-SnO<sub>2</sub> is high which is good for sensing studies as porous sample offer large area for adsorption of gaseous molecule.

Sensing properties of ZnO and ZnO-SnO<sub>2</sub> were analyzed by measuring the resistance in presence of air and carbon

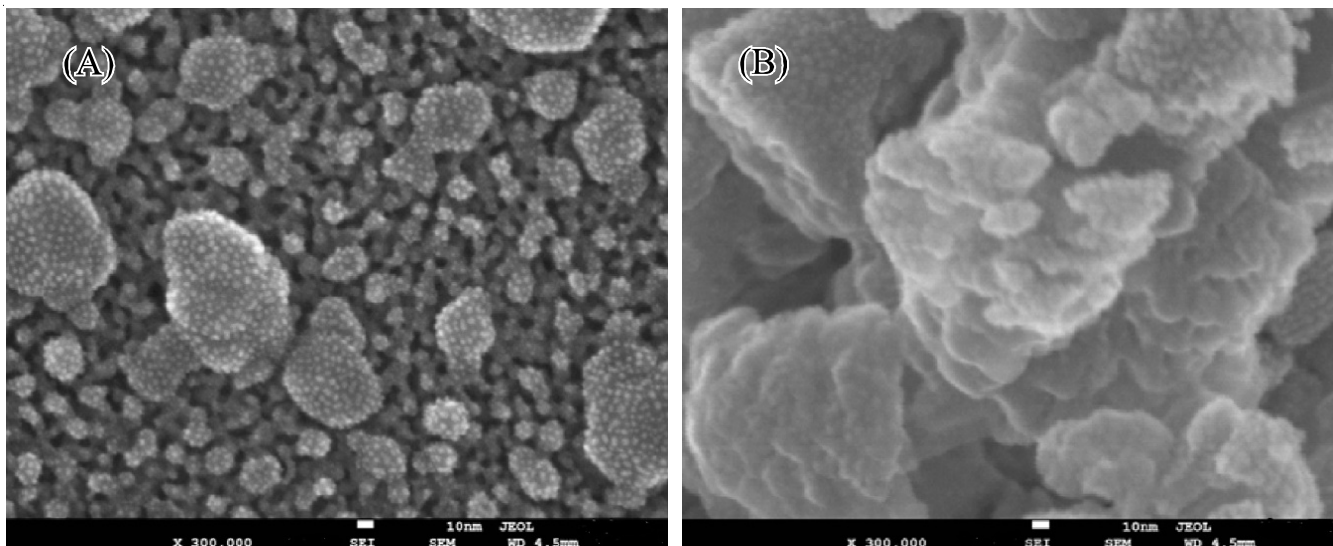


Fig. 3. FE-SEM images of ZnO (A) and ZnO-SnO<sub>2</sub> (B)

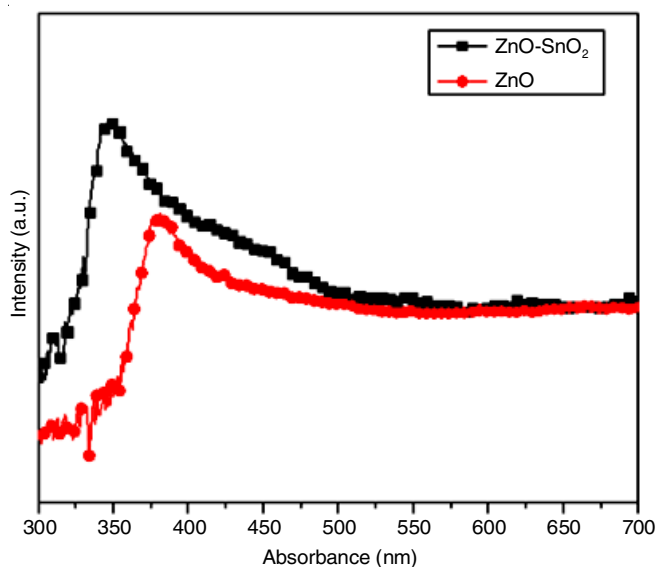


Fig. 2. Absorbance vs. wavelength curves of ZnO and ZnO-SnO<sub>2</sub>

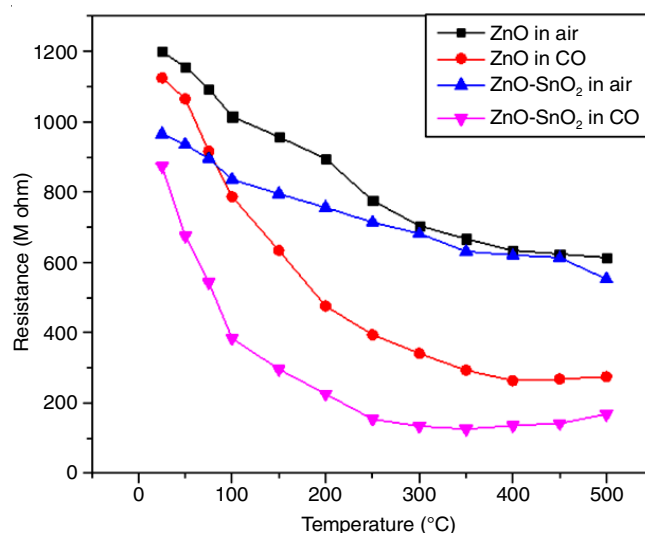
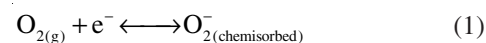


Fig. 4. Resistance vs. operating temperature curves recorded by using ZnO and ZnO-SnO<sub>2</sub> in presence of air and CO gas

monoxide. It was observed that both the materials were highly sensitive to carbon monoxide gas. The resistance of samples at room temperature was very high may be due to presence of hydroxyl ions but at higher temperature, resistance decreased [12]. To investigate the effect of working temperature, resistance was recorded at different temperature. Initially temperature was increased by 25 °C but latter on it was increased by 50 °C. Fig. 4 depicts the variation in resistance at different temperature in presence or air and CO gas. It can be seen that as the temperature was increased, resistance decreased significantly. In the presence of CO gas, resistance decreased remarkably compared to air. At lower temperature, high resistance was recorded which may be attributed to adsorbed water molecule on material surface forming hydroxyls causing formation of positively charge depletion layer [12]. On increasing temperature, these hydroxyl ions get desorbed and therefore resistance decreases. A sharp decrease in resistance can be seen in the presence of CO gas which confirm that prepared materials are highly sensitive to CO gas. On increasing the temperature,

CO molecules become more active and required thermal energy for surface redox reaction to react with surface adsorbed oxygen ions resulting in the formation of CO<sub>2</sub> gas and one electron [11]. Oxygen molecule present in air are adsorbed on the material surface and extract electrons from the conduction band and form anionic oxygenated complex on the surface [22] (eqns. 1 and 2). It leads to decrease in free electron density on ZnO surface forming electron depletion layer that leads to high initial resistance of sensor [23].



When reducing gas come to the contact, negatively charged oxygen ions release electrons and hence resistance decreases. Oxidation of CO to CO<sub>2</sub> produces one free electron which is transferred to bulk material and resistance of material decreases. The mechanism of electronic movement is shown in Fig. 5.

However, at high temperature, decrease in resistance got saturation. In fact, resistance started to increase at higher

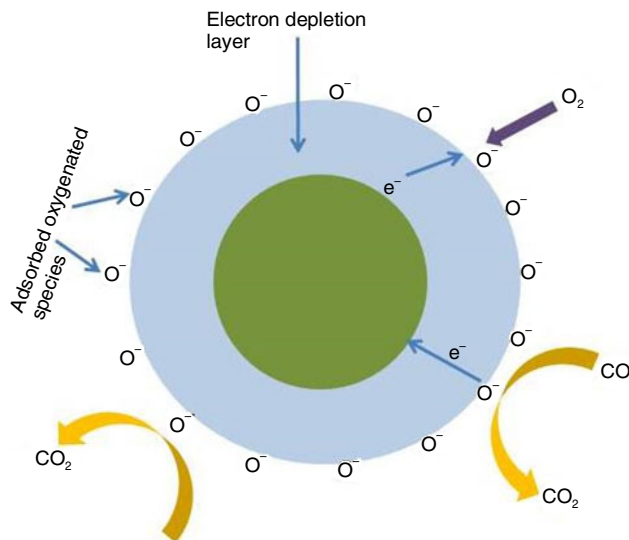


Fig. 5. Sensing mechanism of ZnO-SnO<sub>2</sub>

temperature. This rise in resistance may be attributed to desorption of gaseous molecule as at higher temperature, gaseous molecules get enough kinetic energy for desorption. Working temperature is one of the most crucial factors as high temperature increases the sensor response but at the same time increase in temperature also cause desorption of gaseous molecule. So working temperature must be optimized.

Fig. 6 shows the variation in response of ZnO and Fe-ZnO with temperature. It can be seen that sensing response increased with increase in working temperature. Sensing response of ZnO-SnO<sub>2</sub> is much higher compared to pure ZnO. It was also observed that upto one particular temperature (elevated temperature), response increased and above that temperature response decreased. Oxygen adsorption and surface reaction of analyte gas is temperature dependent and therefore, optimization is required [13]. Although maximum response was recorded in the range of 250-350 °C, sensor response was also good in the range of 150-250 °C. In case of ZnO-SnO<sub>2</sub>, response was high in the range 100-250 °C compared to pure ZnO which may be

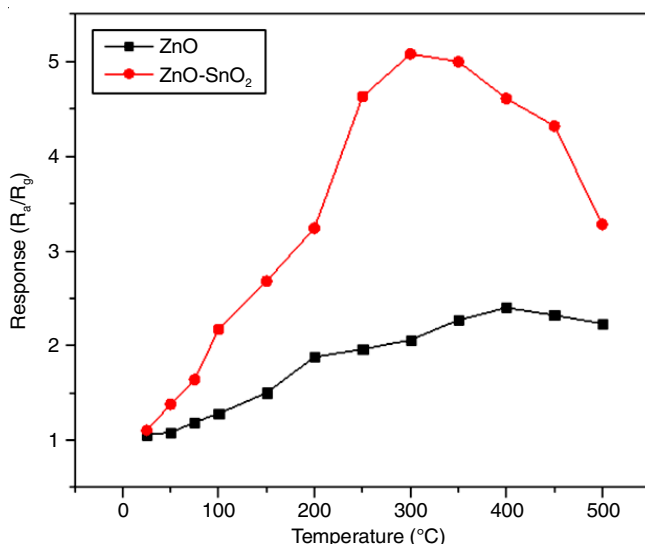


Fig. 6. Sensing response of ZnO and ZnO-SnO<sub>2</sub> at different operating temperature

due to fast charge transfer process. It is reported that if crystal dimension is less than 20 nm, sensor response increases drastically as in this range whole crystal is depleted by gas and when gas is exposed to sensor, resistivity decreases very fast [24].

The response and recovery time were also recorded to investigate the sensing properties of ZnO and ZnO-SnO<sub>2</sub> (Fig. 7). Response time of ZnO was 6.95 s while that of ZnO-SnO<sub>2</sub> was 5.71 s.

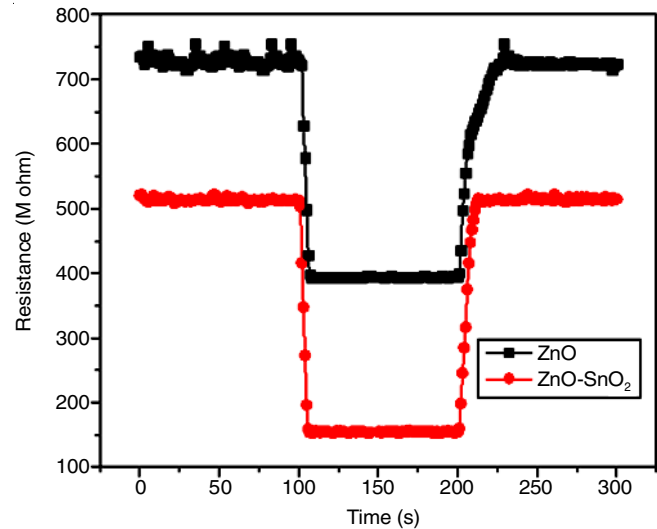


Fig. 7. Sensing transient curves recorded by using ZnO and ZnO-SnO<sub>2</sub> for 100 ppm of CO gas

There is no major difference in response time of both material but in case of ZnO-SnO<sub>2</sub>, response time is less than ZnO. Recovery time of ZnO was 24.76 s while in case of ZnO-SnO<sub>2</sub> recovery time was 13.14 s. Sensing transient curves shows that ZnO-SnO<sub>2</sub> is highly sensitive to CO gas. However, more efforts are required to reduce the response and recovery time.

## Conclusion

Hexagonal wurtzite and rutile phase of ZnO-SnO<sub>2</sub> heterostructure was synthesized by co-precipitation method. Synthesized material was exposed to carbon monoxide gas and sensor response was recorded by measuring change in resistance in the presence of air and CO gas. It was found that sensor sensitivity/sensor response was very high compared to pure ZnO at lower operating temperature (100-250 °C). Response time and recovery time was also reduced.

## CONFLICT OF INTEREST

The authors declare that there is no conflict of interests regarding the publication of this article.

## REFERENCES

1. G. Reumuth, Z. Alharbi, K.S. Houshyar, B.-S. Kim, F. Siemers, P.C. Fuchs and G. Grieb, *Burns*, **45**, 526 (2019); <https://doi.org/10.1016/j.burns.2018.07.006>.
2. A.J. Kulandaisamy, V. Elavalagan, P. Shankar, G.K. Mani, K.J. Babu and J.B.B. Rayappan, *Ceram. Int.*, **42**, 18289 (2016); <https://doi.org/10.1016/j.ceramint.2016.08.156>.
3. S. Das and V. Jayaraman, *Prog. Mater. Sci.*, **66**, 112 (2014); <https://doi.org/10.1016/j.pmatsci.2014.06.003>.

4. K. Mahendraprabhu, A. S. Sharma and P. Elumalai, *Sens. Actuators B: Chem.*, **283**, 842 (2019); <https://doi.org/10.1016/j.snb.2018.11.164>.
5. P. Singh, M. MAbdullah, S. Sagadevan, C. Kaur and S. Ikram, *Optik*, **182**, 512 (2019); <https://doi.org/10.1016/j.ijleo.2019.01.077>.
6. A. Debataraaja, D.W. Zulhendri, B. Yulianto, Nugraha, Hiskia and B. Sunendar, *Procedia Eng.*, **170**, 60 (2017); <https://doi.org/10.1016/j.proeng.2017.03.011>.
7. M. Yin and Z. Zhu, *J. Alloys Compds.*, **789**, 941 (2019); <https://doi.org/10.1016/j.jallcom.2019.03.143>.
8. X. Qiang, M. Hu, L. Zhou and J. Liang, *Mater. Lett.*, **231**, 194 (2018); <https://doi.org/10.1016/j.matlet.2018.08.057>.
9. S. Maeng, S.W. Kim, D.H. Lee, S.E. Moon, K. Kim and A. Maiti, *ACS Appl. Mater. Interfaces*, **6**, 357 (2014); <https://doi.org/10.1021/am404397f>.
10. D. Zappa, V. Galstyan, N. Kaur, H. M. M. M. Arachchige, O. Sisman and E. Comini, *Anal. Chim. Acta*, **1039**, 1 (2018); <https://doi.org/10.1016/j.aca.2018.09.020>.
11. L. Zhu and W. Zeng, *Sens. Actuators A: Phys.*, **267**, 242 (2017); <https://doi.org/10.1016/j.sna.2017.10.021>.
12. A. Umar, J.-H. Lee, R. Kumar and O. Al-Dossary, *Nanosci. Nanotechnol. Lett.*, **8**, 241 (2016); <https://doi.org/10.1166/nnl.2016.2109>.
13. D.R. Miller, S.A. Akbar and P.A. Morris, *Sens. Actuators B: Chem.*, **204**, 250 (2014); <https://doi.org/10.1016/j.snb.2014.07.074>.
14. P Kumar, Samiksha, Shalini and R. Gill, *Asian J. Chem.*, **30**, 2737 (2018); <https://doi.org/10.14233/ajchem.2018.21574>.
15. U.T. Nakate, R. Ahmad, P. Patil, Y. Wang, K.S. Bhat, T. Mahmoudi, Y.T. Yu, E. Suh, and Y.B. Hahn, *J. Alloys Compd.*, **797**, 456 (2019); <https://doi.org/10.1016/j.jallcom.2019.05.111>.
16. T. Wang, X. Kou, L. Zhao, P. Sun, C. Liu, Y. Wang, K. Shimanoe, N. Yamazoe and G. Lu, *Sens. Actuators B Chem.*, **250**, 692 (2017); <https://doi.org/10.1016/j.snb.2017.04.099>.
17. H.A. Khorami, M. Keyanpour-Rad and M.R. Vaezi, *Appl. Surf. Sci.*, **257**, 7988 (2011); <https://doi.org/10.1016/j.apsusc.2011.04.052>.
18. A. Kusior, M. Radecka, M. Rekas, M. Lubecka, K. Zakrzewska, A. Reszka and B.J. Kowalski, *Proc. Eng.*, **47**, 1073 (2012); <https://doi.org/10.1016/j.proeng.2012.09.336>.
19. J.M. Walker, S.A. Akbar and P.A. Morris, *Sens. Actuators B: Chem.*, **286**, 624 (2019); <https://doi.org/10.1016/j.snb.2019.01.049>.
20. S.H. Yan, S.Y. Ma, W.Q. Li, X.L. Xu, L. Cheng, H.S. Song and X.Y. Liang, *Sens. Actuators B: Chem.*, **221**, 88 (2015); <https://doi.org/10.1016/j.snb.2015.06.104>.
21. A. Sahai, Y. Kumar, V. Agarwal, S.F. Olive-Méndez and N. Goswami, *J. Appl. Phys.*, **116**, 164315 (2014); <https://doi.org/10.1063/1.4900721>.
22. F. Ahmed, N. Arshi, M.S. Anwar and B.H. Koo, *J. Nanosci. Nanotechnol.*, **14**, 8590 (2014); <https://doi.org/10.1166/jnn.2014.10008>.
23. S.B. Jagadale, V.L. Patil, S.A. Vanalakarc, P.S. Patil and H.P. Deshmukh, *Ceram. Int.*, **44**, 3333 (2018); <https://doi.org/10.1016/j.ceramint.2017.11.116>.
24. N. Yamazoe, G. Sakai and K. Shimanoe, *Catal. Surv. Asia*, **7**, 63 (2003); <https://doi.org/10.1023/A:1023436725457>.